ELSEVIER

Journal of Organometallic Chemistry 492 (1995) 135–144

Journal of Organometallic Chemistry

Triosmium and triruthenium clusters containing diazaheterocycles

Razaram Agarwala [a], Kazi A. Azam [a], Rahima Dilshad [a], Shariff E. Kabir [a], Rashid Miah [a], Mohammad Shahiduzzaman [a], Kenneth I. Hardcastle [b], Edward Rosenberg [c,*], Michael B. Hursthouse [d], K.M. Abdul Malik [d]

[a] *Department of Chemistry, Jahangirnagar University, Savar, Dhaka 1342, Bangladesh*
[b] *Department of Chemistry, California State University, Northridge, CA 91330, USA*
[c] *Department of Chemistry, The University of Montana, Missoula, MT 59812, USA*
[d] *School of Chemistry and Applied Chemistry, University of Wales Cardiff, Cardiff CF1 3TB, UK*

Received 30 June 1994; in revised form 6 September 1994

Abstract

The reactions of $Os_3(CO)_{11}(MeCN)$ with 1-vinylimidazole, imidazole and pyrazole (L–H) result in the formation of $Os_3(CO)_{11}(L\text{–}H)$ (**1**, L–H = 1-vinylimidazole; **2**, L–H = imidazole; **3**, L–H = pyrazole) in good yields. Thermolysis of these complexes at 98 °C gives two separable isomers of $(\mu\text{-H})Os_3(CO)_{10}(\mu\text{-L})$. In the case of **1** and **2**, these isomers are formed by the activation of the two C–H bonds adjacent to the imino nitrogen atom whereas for **3** they are formed by either a C–H or a N–H activation. These isomers interconvert at 128 °C. The reaction of $Ru_3(CO)_{12}$ with 1-vinyl-imidazole and imidazole in the presence of sodium benzophenone ketyl at 67 °C yields the cyclodimetallated compounds $(\mu\text{-H})Ru_3(CO)_{10}(\mu\text{-}2, 3\text{-}\eta^2\text{-}\overline{C{=}NCH{=}CHN}R)$ (**7**, R = CH=CH$_2$; **8**, R = H) in the same isomeric form as the minor isomers in the osmium series. All the new compounds are characterized by IR, ^{1}H-NMR and elemental analysis together with the X-ray crystal structures of **2** and **7**. Compound **2** crystallizes in the monoclinic space group $P2_1/c$ with unit cell parameters $a = 12.081(2)$ Å, $b = 10.539(2)$ Å, $c = 15.834(2)$ Å, $\beta = 102.61(2)°$, $V = 1959(1)$ Å^3 and $Z = 4$. Least-squares refinement of 3570 reflections gave a final agreement factor of $R = 0.0655$ ($R_w = 0.0728$). Compound **7** crystallizes in the monoclinic space group $P2_1/c$ with unit cell parameters $a = 14.665(4)$ Å, $b = 7.5311(9)$ Å, $c = 18.291(4)$ Å, $\beta = 96.14(1)°$, $V = 2008.5(7)$ Å^3 and $Z = 4$. Least-squares refinement of 3042 reflections gave a final agreement factor of $R = 0.0407$ ($R_w = 0.0749$).

Keywords: Osmium; Heterocycles; Cluster; Diazine; Nitrogen; Hydride

1. Introduction

The activation of C–H and N–H bonds of aliphatic and aromatic nitrogen heterocycles by triosmium and triruthenium clusters has been the subject of numerous studies [1–13]. These ligands may coordinate to the cluster through the nitrogen, by cyclodimetallation of the ring, via a substituent group only or via the nitrogen and the substituent group. The direct reaction of $Os_3(CO)_{12}$ with aromatic nitrogen heterocycles requires pyrolytic conditions and leads to cyclodimetallated products with hydrogen transfer to the triosmium framework [2]. In such reactions, for example pyridine, the first step is believed to occur via carbonyl dissociation, coordination of nitrogen leading to the intermediate (not directly observed) $Os_3(CO)_{11}(\eta^1\text{-NC}_5H_5)$ which then eliminates another CO, followed by oxidative addition of the adjacent C–H bond giving $(\mu\text{-H})Os_3(CO)_{10}(\mu\text{-}\eta^2\text{-NC}_5H_4)$ (Eq. (1)). The postulated intermediate $Os_3(CO)_{11}(\eta^1\text{-NC}_5H_5)$ in the reaction of $Os_3(CO)_{12}$ with pyridine was later synthesized from the reaction of $Os_3(CO)_{11}(MeCN)$ with pyridine and converted into the cyclodimetallated product $(\mu\text{-H})Os_3(CO)_{10}(\mu\text{-}\eta^2\text{-NC}_5H_4)$ by Lewis et al. [1a] (Eq. (2)). The use of lightly stabilized clusters $Os_3(CO)_{10}(MeCN)_2$ and $Os_3(CO)_{10}(C_8H_{14})_2$($C_8H_{14}$ = cyclooctene) to synthesize cyclodimetallated products from a variety of aromatic nitrogen heterocycles such as pyridine [7], substituted pyridines [7], imidazole [5a], pyrazole [5a], 2-pyridone [8] and 2-aminopyridine [8] has also been reported. We report herein the synthesis of a series of initial adducts from the reactions of $Os_3(CO)_{11}(MeCN)$ with the diazacyclopentadiene series:

* Corresponding author.

0022-328X/95/$09.50 © 1995 Elsevier Science S.A. All rights reserved
SSDI 0022-328X(94)05223-9

1-vinylimidazole, imidazole and pyrazole and their subsequent conversion to the cyclodimetallated complexes. We also describe the synthesis of the related cyclodimetallated triruthenium clusters from the reactions of $Ru_3(CO)_{12}$ with 1-vinylimidazole and imidazole respectively using sodium benzophenone ketyl as the reaction promoter.

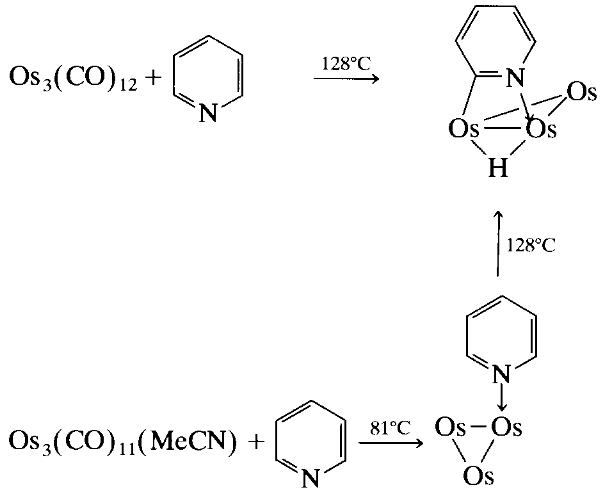

(1)

(2)

2. Results and discussion

Treatment of $Os_3(CO)_{11}(MeCN)$ with 1-vinylimidazole, imidazole and pyrazole readily yields complexes $Os_3(CO)_{11}(\eta^1\text{-}\overline{CH{=}NCH{=}CHN}R)$ (**1**, R = $HC{=}CH_2$; **2**, R = H) and $Os_3(CO)_{11}(\eta^1\overline{CH{=}CHCH{=}NN}H)$ (**3**) in 75, 86 and 60% yield respectively. The infrared spectra of

Table 1
IR and ^{1}H-NMR data for the new compounds

Compound	(CO) [a] (cm^{-1})	^{1}H-NMR [c]
$Os_3(CO)_{11}(\eta^1\text{-}\overline{CH{=}NCH{=}CHN}CH{=}CH_2)$(**1**)	2101w, 2048s, 2033s, 2016m, 2002s, 1998sh 1980sh, 1975m, 1960sh, 1948w	7.68 (overlapping dd, 1H) 7.09 (overlapping dd, 1H) 7.00 (overlapping dd, 1H) 6.84 (dd, J = 8.72 & 15.61, 1H) 5.40 (dd, J = 2.46 & 15.61, 1H) 5.13 (dd, J = 2.46 & 8.72, 1H)
$Os_3(CO)_{11}(\eta^1\text{-}\overline{CH{=}NCH{=}CHN}H)$(**2**)	2098w, 2047s, 2032s, 2015m, 2000s, 1997sh, 1975m, 1960sh, 1948w	9.46 (br, 1H) 7.75 (m, 1H) 7.12 (m, 1H) 6.91 (m, 1H)
$Os_3(CO)_{11}(\eta^1\text{-}\overline{CH{=}CHCH{=}NN}H)$(**3**)	[b] 2100w, 2052s, 2035vs, 2011s, 1999s, 1971m, 1960sh, 1946w	9.96 (br, 1H) 7.68 (overlapping dd, 1H) 7.47 (d, J = 2.78, 1H) 6.29 (overlapping dd, 1H)
$(\mu\text{-}H)Os_3(CO)_{10}(\mu\text{-}3,4\text{-}\eta^2\text{-}\overline{CH{=}NC{=}CHN}CH{=}CH_2)$(**4a**)	2100w, 2061vs, 2050s, 2019vs, 2006s, 1999sh, 1989m, 1972w	7.63 (d, J = 1.13, 1H) 6.60 (d, J = 1.13, 1H) 6.70 (dd, J = 8.78 & 15.63, 1H) 5.19 (dd, J = 2.06 & 15.63, 1H) 4.82 (dd, J = 2.06 & 8.78, 1H) − 15.32 (s, 1H)
$(\mu\text{-}H)Os_3(CO)_{10}(\mu\text{-}2,3\text{-}\eta^2\text{-}\overline{C{=}NCH{=}CHN}CH{=}CH_2)$(**4b**)	2103w, 2063vs, 2053s, 2021s, 2012s, 2003m, 1990m, 1974w	8.86 (d, J = 1.80, 1H) 8.77 (d, J = 1.80, 1H) 6.78 (dd, J = 1.79 & 15.62, 1H) 5.24 (dd, J = 8.87 & 15.62, 1H) 4.98 (dd, J = 1.79 & 8.81, 1H) − 15.05 (s, 1H)
$(\mu\text{-}H)Ru_3(CO)_{10}(\mu\text{-}2,3\text{-}\eta^2\text{-}\overline{C{=}NCH{=}CHN}CH{=}CH_2)$(**7**)	2101w, 2061s, 2050s, 2022s, 2017s, 2005m, 1995m	7.09 (d, J = 1.65, 1H) 6.70 (d, J = 1.65, 1H) 6.94 (dd, J = 1.23 & 13.02, 1H) 5.19 (dd, J = 7.35 & 13.02, 1H) − 14.40 (s, 1H)
$(\mu\text{-}H)Ru_3(CO)_{10}(\mu\text{-}2,3\text{-}\eta^2\text{-}\overline{C{=}NCH{=}CHN}H)$(**8**)	2101w, 2062s, 2052s, 2023s, 2017s, 2005m, 1995m	8.83 (br, 1H) 6.90 (overlapping dd, 1H) 6.70 (overlapping dd, 1H) − 14.50 (s, 1H)

[a] Recorded in hexane unless stated otherwise.
[b] In dichloromethane.
[c] Recorded in $CDCl_3$; J in Hz.

1–3, in the carbonyl stretching region, are very similar to those of $Os_3(CO)_{11}(\eta^1\text{-}NC_5H_5)$ [1a]. The ^{1}H-NMR spectra of **1–3** shows well-separated resonances in the 0–10 ppm region for all the protons of the organic ligand (Table 1).

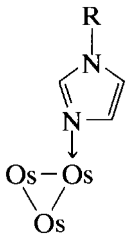

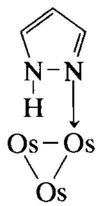

1 R = CH = CH_2
2 R = H
3

For **1** there are six resonances while for each of **2** and **3** there are four resonances each integrating as one hydrogen atom. Thus, the ^{1}H-NMR, infrared and elemental analysis of **1–3** are consistent with the proposed molecular formula. The exact disposition of the heterocyclic ligand could not be ascertained from these data and so a solid state structure determination of **2** was undertaken. Although the pyridine [1a] and ammonia [14] analogs of **1–3** have been reported, no solid state structure of these initial adducts have been reported to date. The structure of **2** is shown in Fig. 1, crystal data are given in Table 2, selected bond distances and angles in Table 3, and atomic coordinates are in Table 4. Compound **2** has an approximate isosceles triangle of osmium atoms with two slightly elongated edges (Os1–Os2 = 2.880(1) and Os1–Os3 = 2.881(1) Å) and one slightly shorter edge (Os2–Os3 = 2.861(1) Å) compared to the average Os–Os bond length of 2.877(1) Å in $Os_3(CO)_{12}$ [15]. The elongated Os–Os bonds are associated with the metal atom which is coordinated to the imidazole ligand. This is in contrast to that observed for the mono-acetonitrile compound

Table 2
Crystallographic data for **2** and **7**

Compound	**2**	**7**
Formula	$C_{14}H_4N_2O_{11}Os_3$	$C_{15}H_6N_2O_{10}Ru_3$
Formula weight	946.79	677.43
Crystal dimensions, mm^3	0.15 × 0.20 × 0.25	0.10 × 0.08 × 0.04
Radiation, wavelength, Å	Mo, 0.71073	Mo, 0.71069
Temperature, °K	298 ± 1	150 ± 2
Crystal System	monoclinic	monoclinic
Space group	$P2_1/c$	$P2_1/c$
a, Å	12.031 (2)	14.665 (4)
b, Å	10.539 (2)	7.5311 (9)
c, Å	15.834 (4)	18.291 (4)
β, deg	102.61 (2)	96.142 (12)
V, Å^3	1959 (1)	2008.5 (7)
Z	4	4
F(000)	1672	1288
Density, g cm^{-3}	3.21	2.24
Absorption coeff. μ, cm^{-1}	195.0	21.03
Rel. transmission coeff.	0.610–0.987	0.926–1.112
hkl ranges	h: −15 to 15	h: −17 to 17
	k: 0 to 13	k: −4 to 8
	l: 0 to 20	l: −21 to 21
2θ range, deg	4.0–56.0	–
θ range, deg	–	2.2–25.1
Structure solution	Patterson method	Patterson method
No. of data collected	4957	7043
No. of unique data	4957	3042
No. of data used	3570	3042
in L.S. refinement	$(F_o > 3.0\sigma(F_o))$	$(F_o > 0)$
Weighting scheme, w	$4F_o^2/[\sigma(F_o)^2]^2$	$1/[\sigma^2(F_o)^2 + (0.035P^*)^2]$
No. of parameters refined	271	280
R [a]	0.0655 [a]	0.0327 [a]
R_w [b,c]	0.0728 [b]	0.0749 [c]
Esd of obs. of unit weight (GOF)	1.03	0.964
Largest shift/esd	0.04	0.01
Highest peak in final diff. map, e Å^3	2.17 (50)	1.137

[a] $R = \Sigma[\,|F_o| - F_c|]/\Sigma|F_o|$.
[b] $R_w = [\Sigma w(|F_o| - |F_c|)^2/\Sigma w|F_o|^2]^{1/2}$.
[c] $R_w = [\Sigma\{w(\Delta F^2)^2\}/\Sigma\{w(F_o^2)^2\}]^{1/2}$.
* $P = (F_o^2 + 2F_c^2)/3$.

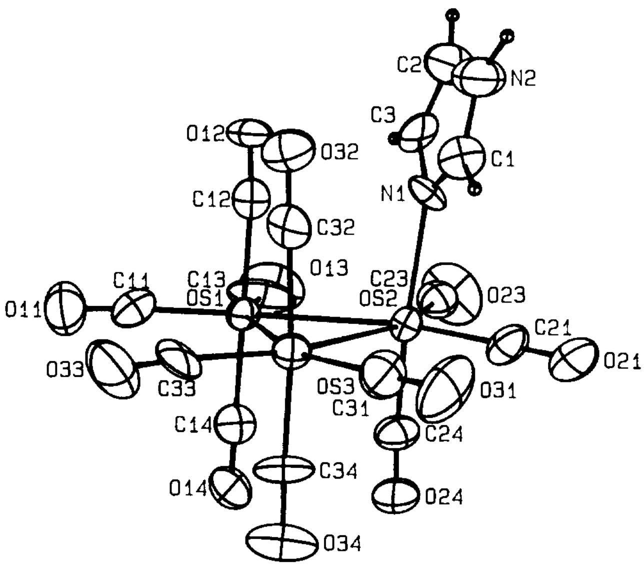

Fig. 1. An ORTEP diagram of $OS_3(CO_{11}(\eta\text{-}\overline{CH{=}NCH{=}CHN}H)(\mathbf{2})$.

Table 3
Selected bond distances (Å) and angles (deg) for **2** [a]

Distances			
Os1–Os2	2.880(1)	N1–C1	1.32(3)
Os1–Os3	2.881(1)	N1–C3	1.33(3)
Os2–Os3	2.861(1)	N2–C1	1.31(4)
Os2–N1	2.23(2)	C2–C3	1.34(4)
Os–C(CO)	1.92(2) [b]		
C–O(CO)	1.14(3) [b]		
Angles			
Os2–Os1–Os3	59.55(3)	C1–N1–C3	104.(2)
Os1–Os2–Os3	60.25(3)	N1–C3–C2	110.(3)
Os1–Os3–Os2	60.20(3)	N1–C1–N2	114.(2)
Os1–Os2–N1	97.9(5)	C1–N2–C2	105.(3)
Os–C–O(CO)	176(2) [b]	C3–C2–N2	107.(3)

[a] Numbers in parentheses are estimated standard deviations in the least significant digits.
[b] Average values.

$Os_3(CO)_{11}(MeCN)$ in which the Os–Os bonds associated with the metal atom to which the acetonitrile is coordinated are shorter (2.856(2) and 2.861(2) Å) [16]. The imidazole ligand is coordinated through the imino nitrogen atom and occupies an axial coordination site on Os2. The Os2–N1 bond length in **2** (2.23(2) Å) is very similar to the Os–N bond length in $(\mu\text{-}H)_2Os_5(CO)_{14}(\eta^1\text{-}C_5H_5N)$ (2.214(22) Å) [17]. Both are significantly longer than the Os–N bond length in $Os_3(CO)_{11}(MeCN)$(2.074(23) Å).

Thermolysis of **1** and **2** in heptane at 98 °C yields two isomeric compounds $(\mu\text{-}H)Os_3(CO)_{10}(\mu\text{-}3,4\text{-}\eta^2\text{-}\overline{CH{=}NC{=}CHN}R)$ (**4a**, R = CH=CH$_2$, 40%; **5a**, R = H, 45%) and $(\mu\text{-}Os_3(CO)_{10}(\mu\text{-}2,3\text{-}\eta^2\text{-}\overline{C{=}NCH{=}CHN}R)$ (**4b**, R = CH=CH$_2$, 21%; **5b**, R = H, 20%) formed by the activation of one of the two C–H bonds adjacent to the imino nitrogen atom (Eq. (3)).

Compounds **5a** and **5b** have previously been reported by Shapley et al. from the reaction of $Os_3(CO)_{10}(MeCN)_2$ with imidazole at 80 °C [5a]. The structural assignments of **4a** and **4b** were made by comparison of the ^{1}H-NMR and infrared spectroscopic data with those of **5a** and **5b**. The infrared spectra of **4a** (major isomer) and **4b** (minor isomer) are very similar to those of **5a** and **5b**, indicating that they are isostructural [5a]. The ^{1}H-NMR spectrum of the major isomer shows a singlet hydride resonance at −15.32 ppm and two doublets at 7.63 and 6.60 ppm and three doublets of doublets at 6.70, 5.19 and 4.82 ppm. The doublets of doublets at 6.70, 5.19 and 4.82 ppm are assignable to vinylic protons while the doublets at 7.63 and 6.60 ppm are assignable to the C(2)–H and C(5)–H ring protons respectively. Thus, the major isomer does not contain the expected resonances for C(4)–H which suggests that it has structure **4a**. The ^{1}H-NMR spectrum of the minor isomer shows a singlet resonance at −15.05 ppm, two doublet resonances at 6.86 and 6.77 ppm assignable to the C(4)–H and C(5)–H ring protons and three doublets of doublets at 6.78, 5.24 and 4.98 ppm for the vinylic protons. Thus, in contrast to the major isomer, the minor isomer has resonances for C(4)–H but not for the C(2)–H which implies it has structure **4b**. The previous structural study of **5a** and **5b** suffered from a disorder problem around the osmium–nitrogen and osmium–carbon bonds [5a,b] and we also failed to obtain X-ray quality crystals of **4a** and **4b** for X-ray analysis but we were able to obtain X-ray quality crystals of a ruthenium analog of **4b** which

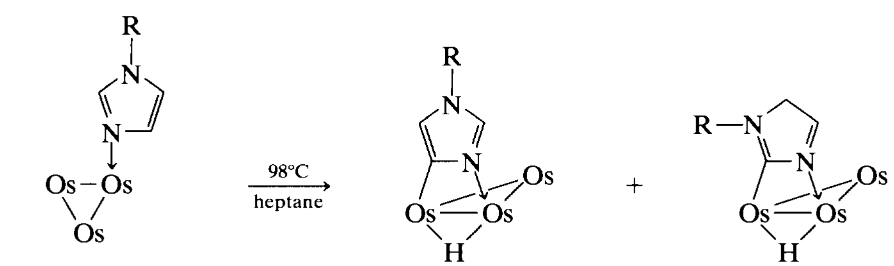

(3)

1 R = CH = CH$_2$
2 R = H

4a R = CH = CH$_2$
5a R = H

4b R = CH = CH$_2$
5b R = H

Table 4
Fractional atomic coordinates for **2**

Atom	x	y	z	B(A2)
OS1	0.37300(7)	0.11453(8)	0.76809(5)	2.60(1)
OS2	0.14313(7)	0.09589(9)	0.79220(5)	2.49(1)
OS3	0.30987(7)	0.23331(8)	0.91468(5)	2.55(1)
O11	0.627(2)	0.179(2)	0.809(1)	5.9(5)
O12	0.427(2)	−0.139(2)	0.861(1)	4.4(4)
O13	0.324(2)	−0.031(2)	0.597(1)	7.3(6)
O14	0.327(2)	0.367(2)	0.668(1)	5.0(4)
O21	−0.073(2)	0.140(2)	0.858(1)	5.4(5)
O23	0.047(2)	−0.059(3)	0.632(1)	7.5(7)
O31	0.131(2)	0.299(2)	1.021(1)	6.3(5)
O32	0.379(2)	−0.014(2)	1.014(1)	4.1(4)
O33	0.532(2)	0.351(2)	1.013(2)	7.0(6)
O34	0.258(2)	0.484(2)	0.819(1)	5.9(6)
N1	0.165(2)	−0.080(2)	0.872(1)	2.8(3)
N2	0.148(2)	−0.212(2)	0.977(2)	5.5(6)
C1	0.145(2)	−0.093(2)	0.951(1)	3.4(5)
C2	0.176(3)	−0.279(3)	0.912(2)	5.0(7)
C3	0.189(2)	−0.197(2)	0.850(2)	4.2(6)
C11	0.531(2)	0.150(2)	0.792(1)	3.3(5)
C12	0.402(2)	−0.046(2)	0.792(1)	2.9(4)
C13	0.344(4)	0.022(3)	0.661(2)	6.6(9)
C14	0.344(2)	0.275(2)	0.708(1)	3.5(5)
C21	0.010(2)	0.122(2)	0.834(2)	3.5(5)
C23	0.082(2)	−0.010(3)	0.693(2)	4.2(6)
C24	0.113(2)	0.247(3)	0.725(2)	3.9(5)
C31	0.200(2)	0.275(3)	0.981(2)	4.0(5)
C32	0.354(2)	0.078(2)	0.975(1)	3.2(4)
C33	0.454(2)	0.304(2)	0.977(2)	4.1(5)
C34	0.280(3)	0.386(2)	0.849(2)	4.2(6)
H1	0.129	−0.024	0.984	4.3 *
H2	0.185	−0.369	0.910	6.3 *
H3	0.211	−0.218	0.798	5.5 *
H4	0.134	−0.243	1.030	7.1 *

Starred atoms were refined isotropically.
Anisotropically refined atoms are given in the form of the isotropic equivalent displacement parameter defined as:
(4/3)*[a2*B(1,1)+b2*B(2,2)+c2*B(3,3)+ab(cos gamma)*B(1,2) +ac(cos beta)*B(1,3)+bc(cos alpha)*B(2,3)].

enabled us to establish its structure (vide infra). Compounds **4a** and **4b** may also be obtained in 45 and 18% yields from the reaction of $Os_3(CO)_{10}(MeCN)_2$ with 1-vinylimidazole at 50–60 °C (Eq. (4)).

Thermolysis of **3** in heptane at 98 °C gives (μ-H)$Os_3(CO)_{10}$(μ-1, 2-η^2-CH=CHCH=NN) (**6a**) and (μ-H)$Os_3(CO)_{10}$(μ-2, 3-η^2-C=CHCH=NNH) (**6b**) in 38 and 11% yields respectively (Eq. (5)).

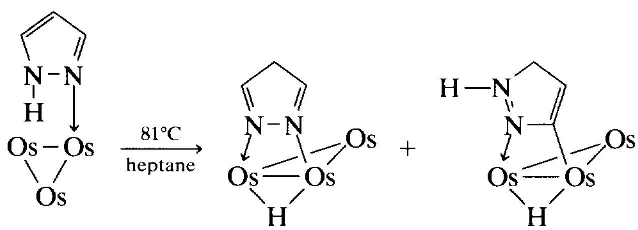

3 6a 6b (5)

The major isomer is formed by the activation of N–H bond while the minor one is formed by C(3)–H bond activation. Shapley and coworkers reported compounds **6a** and **6b** from the reaction of $Os_3(CO)_{10}$-$(MeCN)_2$ with pyrazole at 80 °C and we have characterized these two compounds by comparing the infrared and ^{1}H-NMR spectroscopic data with those reported [5a].

Thermolysis of the major isomers **4a** and **5a** at 128 °C for 8 h results in partial conversion to the minor isomer **4b** (32%) or **5b** (30%) as well as considerable decomposition. Similarly, thermolysis of the minor isomers gives the major isomers (**4a**, 13%; **5a**, 16%) although more slowly and in lower yields. These results are in accord with Shapley's earlier results in that the isomer distribution for **4** and **5** is kinetically determined. However, we found that at least at 128 °C, structures **4a** and **4b** and **5a** and **5b** do indeed inconvert.

In contrast to the extensive nitrogen derivative chemistry (simple substitution, carbon–hydrogen and carbon nitrogen activations) of triosmium clusters, relatively few such derivatives of $Ru_3(CO)_{12}$ containing nitrogen donor ligands have been reported. This may be due to the forcing reaction conditions required for the formation of such compounds leading to the break-up of triruthenium framework resulting in the formation of di and tetranuclear complexes. However, nitrogen containing heterocycles such as pyridine, [3,10] quinoline [3], pyridazine [11], pyrazole [10,13] and ben-

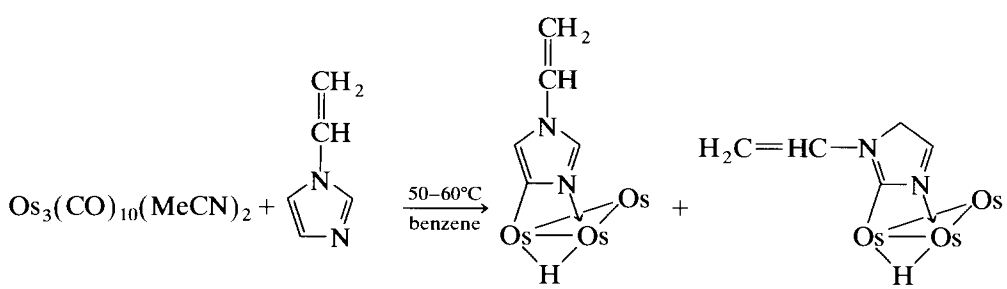

4a 4b (4)

Table 5
Selected bond distances (Å) and angles (deg) for **7** [a]

Distances			
Ru1–Ru2	2.8523(7)	N1–C11	1.384(7)
Ru1–Ru3	2.9464(8)	N1–C12	1.397(6)
Ru2–Ru3	2.8494(7)	N2–C11	1.324(6)
Ru1–H1	1.80(6)	N2–C13	1.369(6)
Ru3–H1	1.66(6)	C12–C13	1.360(8)
Ru3–N2	2.108(4)	C14–C15	1.299(8)
Ru1–C11	2.074(5)	C–O(CO)	1.131(7) [b]
Ru–C(CO)	1.925(6) [b]		
Angles			
Ru2–Ru1–Ru3	58.84(2)	C11–N1–C12	108.8(4)
Ru3–Ru2–Ru1	62.23(2)	N2–C11–N1	106.6(4)
Ru2–Ru3–Ru1	58.93(2)	C11–N2–C13	110.4(4)
Ru–C–O(CO)	176.5(5) [b]	C12–C13–N2	108.5(4)
Ru3–Ru1–C1	114.8(2)	C13–C12–N12	124.9(6)
Ru1–Ru3–C8	115.5(2)		

[a] Numbers in parentheses are estimated standard deviations in the least significant digits.
[b] Average values.

zimidazole [12] are exceptions giving substitution or cyclodimetallated triruthenium clusters. In light of the lack of success in obtaining structural quality crystals for **4a** and **4b**, we decided to investigate the reactions of the same ligands with $Ru_3(CO)_{12}$. The reaction of 1-vinylimidazole or imidazole with $Ru_3(CO)_{12}$ in the presence of sodium benzophenone ketyl at 67 °C in THF produces the trinuclear clusters $(\mu\text{-H})Ru_3(CO)_{10}$-$(\mu\text{-}2,3\text{-}\eta^2\text{-}\overline{C{=}NCH{=}CHN}R)$ (**7**, R = CH=CH$_2$, 22%; **8**, R = H, 30%) as the only products (Eq. (6)).

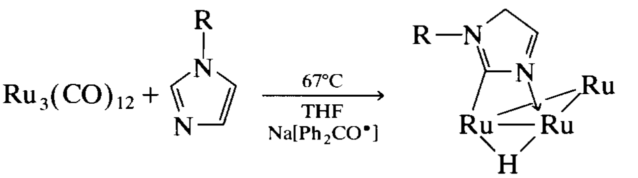

7 R = CH = CH$_2$
8 R = H

(6)

The infrared spectra of **7** and **8** in the carbonyl stretching region are very similar to that reported for $(\mu\text{-H})Ru_3(CO)_{10}(\mu$-benzimidazole) which indicated the presence of terminal carbonyl ligands and the absence of bridging carbonyl groups [12]. The ^{1}H-NMR spectrum of **7** shows a singlet hydride resonance at −14.40 ppm and two doublets at 7.09 and 6.70 ppm for the C(4)–H and C(5)–H ring protons and three doublets of doublets at 6.94, 5.19 and 4.92 ppm for the vinylic protons. The ^{1}H-NMR spectrum of **8** contains a singlet hydride resonance at −14.50 ppm, a broad singlet NH resonance at 8.83 ppm and two apparent triplets (overlapping doublets of doublets) at 6.90 and 6.70 ppm which are assignable to the C(4)–H and C(5)–H ring protons indicating both **7** and **8** are formed by the oxidative addition of C(2)–H bonds with concomitant loss of two CO groups. These results contrast with those obtained from the reaction of $Os_3(CO)_{10}(MeCN)_2$ with 1-vinylimidazole and imidazole which gives two isomeric compounds. Indeed, all of the reactions of $Ru_3(CO)_{12}$ with the pyrazole and imidazole family heterocycles give only one product with the C(2)–H bond activated [10,12]. It is interesting to note that the minor isomer observed in triosmium clusters becomes the only product in triruthenium systems.

In light of the fact that at 128 °C the major isomers **4a** and **5a** isomerize more rapidly to **4b** and **5b** and are then isolated in better yield than for the reverse conversion which is slower, it is tempting to propose that **4b, 5b, 7** and **8** are the thermodynamic products in these reactions. The more rapid C–H oxidative addition-reductive elimination expected for the ruthenium cases **7** and **8** would rationalize these results. The question remains, however, why is the C(2)–H activated product the more thermodynamically stable one. Shapley et al. have suggested that C–H acidity is the reason.

Although the structure of **7** and **8** were clear from their NMR data there are relatively few examples of nitrogen heterocycles bound to $Ru_3(CO)_{10}$ fragments in the literature [3]. We therefore undertook a single crystal X-ray diffraction study of **7**. The structure of **7** is shown in Fig. 2, the crystal data are summarized in Table 2, selected bond distances and angles are presented in Table 5 and fractional atomic coordinates are listed in Table 6. The structure consists of a triruthenium core with two almost equivalent metal–metal bonds (Ru1–Ru2 = 2.8523(7) Å and Ru2–Ru3 = 2.8494(7) Å) and one elongated metal–metal bond (Ru1–Ru3 = 2.9464(8) Å). The organic ligand and the hydride both bridge the elongated metal–metal edge with the hydride lying 0.59 Å below the plane of the metals. The organic η^2-ligand donates 3 electrons via a

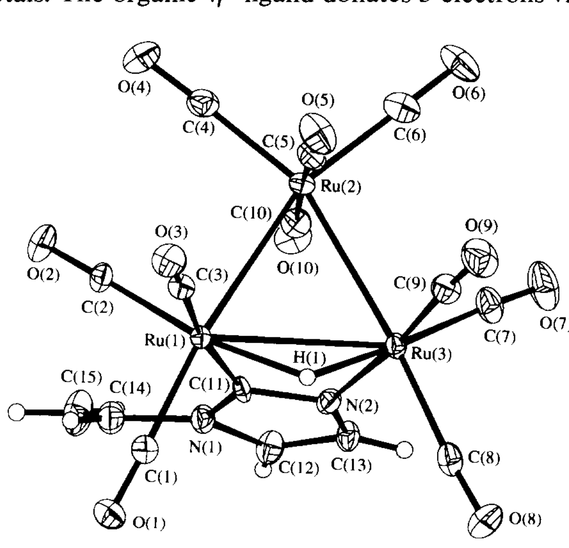

Fig. 2. An ORTEP diagram of $(\mu\text{-}2,3\text{-}\eta^2\text{-}\overline{CH{=}NCH{=}CHN}CH{=}CH_2)$(**7**).

2 electron lone pair donor bond from N2 to Ru3 (N2–Ru3 = 2.108(4) Å) and a one electron sigma bond from C11 to Ru1 (C11–Ru1 = 2.074(5) Å). The structure is derived from that of $Ru_3(CO)_{12}$ by replacement of two axial CO groups on adjacent ruthenium atoms by the 1-vinylimidazolide group and the remaining ten carbonyl groups are all terminal. The maximum deviation from linearity is found for Ru2–C10–O10 (173.3(5) Å) where C10–O10 is the axial CO lying on the same side of the ruthenium triangle as the 1-vinylimidazolide ligand. The structure is comparable to those of (μ-H)$Ru_3(CO)_{10}$(μ-1,2-η^2-$\overline{C(CF_3)CHC(CF_3)NN}$) [10] and ($\mu$-H)$Ru_3(CO)_{10}$($\mu$-$\eta^2$-phenanthridine) [3b] in both of which the hydride and the organic ligand bridges the same Ru–Ru edge. Within their standard deviations, Ru3–N2 (2.108(4) Å vs. 2.133(1) Å), Ru1–C11 (2.075(6) Å vs. 2.133(1) Å and N2–C11 (1.324(6) Å vs. 1.312(0) Å) bond lengths are the same but the Ru–Ru edge spanned by the two bridging ligand is somewhat longer (2.9464(8) Å vs. 2.866(1) Å) than those reported for the related phenanthridine cluster [3b]. These bond parameters are also similar to those reported for the μ-imidoyl triosmium and triruthenium clusters [4].

3. Experimental section

All reactions were performed under an atmosphere of nitrogen. Dichloromethane was distilled from CaH_2 and hexane from sodium benzophenone ketyl before use. Infrared spectra were recorded on a Perkin-Elmer 1420 spectrophotometer. ^{1}H-NMR spectra were recorded on either a Bruker AC-200, AMX-360 or Varian Unity Plus 400 spectrometers. The clusters $Os_3(CO)_{11}(MeCN)$ and $Os_3(CO)_{10}(MeCN)_2$ were prepared by the published procedure [1a]. 1-Vinylimidazole, imidazole and pyrazole were purchased from Aldrich and used as received. Sodium benzophenone ketyl was prepared according to the known procedure[18].

3.1. Reaction of $Os_3(CO)_{11}(MeCN)$ with 1-vinylimidazole

A solution of $Os_3(CO)_{11}(MeCN)$ (0.150 g, 0.163 mmol) and 1-vinylimidazole (32 μl, 0.326 mmol) in $CHCl_3$ (30 ml) was stirred at room temperature for 8 h. The solvent was removed under vacuum and the residue

Table 6
Fractional atomic coordinates for **7**

	x	y	z	U_{eq}
Ru(1)	7858.8(3)	473.9(5)	8147.6(2)	17.7(1)
Ru(2)	6740.0(3)	3447.0(6)	8422.9(2)	20.0(1)
Ru(3)	6913.5(3)	672.4(6)	9487.9(2)	19.8(1)
O(1)	9088(3)	−2765(6)	8039(2)	43(1)
O(2)	8790(3)	2919(6)	7138(2)	41(1)
O(3)	6388(3)	−804(5)	6928(2)	38(1)
O(4)	7085(3)	5503(6)	7039(2)	49(1)
O(5)	5079(3)	1645(6)	7559(2)	44(1)
O(6)	5468(3)	5890(6)	9176(2)	49(1)
O(7)	6549(4)	3254(6)	10700(2)	55(1)
O(8)	6997(3)	−2665(6)	10455(2)	45(1)
O(9)	4897(3)	−35(6)	9064(3)	50(1)
O(10)	8380(3)	5202(5)	9341(2)	36(1)
N(1)	9599(3)	1818(6)	9243(2)	25(1)
N(2)	8325(3)	1232(6)	9700(2)	23(1)
C(1)	8620(4)	−1577(8)	8086(3)	29(1)
C(2)	8434(4)	1999(8)	7507(3)	27(1)
C(3)	6912(4)	−319(7)	7372(3)	27(1)
C(4)	6944(4)	4770(7)	7558(3)	31(1)
C(5)	5710(4)	2234(8)	7886(3)	30(1)
C(6)	6932(4)	4997(8)	8895(3)	33(1)
C(7)	6645(4)	2300(8)	10234(3)	34(1)
C(8)	7014(4)	−1423(8)	10105(3)	30(1)
C(9)	5657(4)	260(7)	9201(3)	30(1)
C(10)	7797(4)	4453(7)	9013(3)	28(1)
C(11)	8701(4)	1263(6)	9074(3)	18(1)
C(12)	9748(4)	2171(7)	9996(3)	30(1)
C(13)	8944(4)	1785(7)	10268(3)	26(1)
C(14)	10254(4)	2075(8)	8741(3)	32(1)
C(15)	10940(5)	3173(9)	8835(3)	49(2)

was dissolved in a minimum of CH_2Cl_2. Chromatography by TLC on silica gel eluting with hexane/CH_2Cl_2(10:3, v/v) gave two bands. The faster moving band gave too small an amount for complete characterization. The second band gave $Os_3(CO)_{11}(\eta^1$-CH=NCH=CHNCH=CH$_2$) (**1**) as yellow crystals (0.119 g, 75%) from hexane/CH_2Cl_2 at −20 °C. Anal. Calc. for $C_{16}H_6N_2O_{11}Os_3$: C, 19.75; H, 0.62; N, 2.88. Found: C, 19.87; H, 0.70; N, 2.88.

3.2. Reaction of $Os_3(CO)_{11}(MeCN)$ with imidazole

A reaction, similar to that above of $Os_3(CO)_{11}$(MeCN) (0.190 g, 0.207 mmol) with imidazole (0.028 g, 0.411 mmol) in $CHCl_3$ (40 ml) followed by similar chromatographic separation yielded $Os_3(CO)_{11}(\eta^1$-CH=NCH=CHNH) (**2**) as yellow crystals from hexane/CH_2Cl_2 at −20 °C (0.165 g, 86%). Anal. Calc. for $C_{14}H_4N_2O_{11}Os_3$: C, 17.76; H, 0.43; N, 2.96. Found: C, 17.95; H, 0.56; N, 3.10.

3.3. Reaction of $Os_3(CO)_{11}(MeCN)$ with pyrazole

A reaction, similar to that above of $Os_3(CO)_{11}$-(MeCN) (0.095 g, 0.103 mmol) with pyrazole (0.014 g, 0.206 mmol) in $CHCl_3$ (30 ml) for 1 h at 0 °C followed by similar chromatographic separation gave $Os_3(CO)_{11}$-(η^1-CH=CHCH=NNH) (**3**) as yellow crystals from hexane/CH_2Cl_2 at −20 °C (0.066 g, 65%). Anal. Calc. for $C_{14}H_4N_2O_{11}Os_3$: C, 17.76; H, 0.43; N, 2.96. Found: C, 17.95; H, 0.65; N, 3.15.

3.4. Thermolysis of $Os_3(CO)_{11}(\eta^1$-CH=NCH=CHNCH=CH$_2$) (1)

A heptane solution (30 ml) of **1** (0.065 g, 0.067 mmol) was heated to reflux for 2 h. The solvent was removed under vacuum, and the residue was chromatographed by TLC on silica gel. Elution with a hexane/CH_2Cl_2(10:3, v/v) gave four bands from which the following compounds were isolated (in order of elution): $Os_3(CO)_{12}$ (0.006 g, 10%), (μ-H)$Os_3(CO)_{10}$-(μ-2, 3-η^2-C=NCH=CHNCH=CH$_2$) (**4b**) as yellow crystals from hexane/CH_2Cl_2 at −20 °C (0.013 g, 21%. Anal. Calcd for $C_{15}H_6N_2O_{10}Os_3$: C, 19.07; H, 0.64; N, 2.97. Found: C, 19.25; H, 0.74; N, 3.05), (μ-H)$Os_3(CO)_{10}$(μ-3,4-η^2-CH=NC=CHNCH=CH$_2$) (**4a**) as yellow crystals from hexane CH_2Cl_2 at −20 °C (0.025 g, 40%. Anal. Calc. for $C_{15}H_6N_2O_{10}Os_3$: C, 19.07; H, 0.64; N, 2.97. Found: C, 19.14; H, 0.75; N, 2.98), and unconsumed **1** (0.013 g).

3.5. Thermolysis of $Os_3(CO)_{11}(\eta^1$-CH=NCH=CHNH) (2)

A similar thermolysis of **2** (0.050 g, 0.053 mmol) in heptane (40 ml) for 2 h followed by similar chromatographic separation gave $Os_3(CO)_{12}$ (0.005 g, 10%), (μ-H)$Os_3(CO)_{10}$(μ-2,3-η^2-C=NCH=CHNH) (**5b**) as yellow crystals from hexane/CH_2Cl_2 at −20 °C (0.010 g, 20%), (μ-H)$Os_3(CO)_{10}$(μ-3,4-η^2-CH=NC=CHNH) (**5a**) as yellow crystals from hexane/CH_2Cl_2 at −20 °C (0.022 g, 45%), and unconsumed **2** (0.010 g).

3.6. Thermolysis of $Os_3(CO)_{11}(\eta^1$-CH=CHCH=NNH) (3)

A similar thermolysis of **3** (0.060 g, 0.063 mmol) in heptane (50 ml) for 2 h followed by similar chromatographic separation gave the following compounds in (order of elution): $Os_3(CO)_{12}$(0.006 g, 11%) (μH)Os_3-$(CO)_{10}$(μ-1, 2-η^2-CH=CHCH=NN) (**6a**) as yellow crystals from hexane/CH_2Cl_2 at −20 °C (0.022 g, 38%), (μ-H)$Os_3(CO)_{10}$(μ-2, 3-η^2-C=CHCH=NNH) (**6b**) as yellow crystals from hexane/CH_2Cl_2 at −20 °C (0.009 g, 16%), and unconsumed **3** (0.008 g).

3.7. Thermolysis of (μ-H)$Os_3(CO)_{10}$(μ-3,4-η^2-CH=NC=CHNCH=CH$_2$) (4a)

An octane solution (30 ml) of **4a** (0.025 g, 0.026 mmol) was heated to reflux for 8 h. The solvent was removed under reduced pressure and the residue was chromatographed by TLC on silica gel. Elution with hexane/CH_2Cl_2 (10:2, v/v) gave three bands. The first band was characterized as $Os_3(CO)_{12}$ (0.003 g, 13%). The second band was characterized as (μ-H)-$Os_3(CO)_{10}$(μ-2,3-η^2-C=NCH=CHNCH=CH$_2$) (**4b**) (0.008 g, 32%). The third band gave unconsumed **4a** (0.007 g, 28%).

3.8. Thermolysis of (μ-H)$Os_3(CO)_{10}$(μ-3,4-η^2-CH=NC=CHNCH=CH$_2$) (4b)

A similar thermolysis of **4b** (0.030 g, 0.032 mmol) to that above of **4a** followed by similar chromatographic workup gave $Os_3(CO)_{12}$ (0.003 g, 10%), unconsumed starting material (0.015 g, 50%) and (μ-H)$Os_3(CO)_{10}$-(μ-3, 4-η^2-CH=NC=CHNCH=CH$_2$) (**4a**) (0.004 g, 13%).

3.9. Thermolysis of (μ-H)$Os_3(CO)_{10}$(μ-3,4-η^2-CH=NC=CHNH) (5a)

This thermolysis was carried out in the same way as for **4a** and **4b** above to give $Os_3(CO)_{12}$ (0.003 g, 10%), (μ-H)$Os_3(CO)_{10}$(μ-2,3-η^2-C=NCH=CHNH) (**5b**) (0.009 g, 30%) and unconsumed starting material (0.007 g, 23%).

3.10. Thermolysis of (μ-H)$Os_3(CO)_{10}$(μ-2,3-η^2-C=NCH=CHNH) (5b)

A similar thermolysis of **5b** (0.025 g, 0.027 mmol) in octane (30 ml) to that above for **5a** for 8 h gave

$Os_3(CO)_{12}$ (0.002 g, 8%), unconsumed (0.012 g, 48%) and (μ-H)$Os_3(CO)_{10}$(μ-3,4-η^2-$\overline{\text{CH=NC=CHNH}}$) (**5a**) (0.004 g, 16%).

3.11. Reaction of $Os_3(CO)_{10}(MeCN)_2$ with 1-vinylimidazole

1-Vinylimidazole (42 μl, 0.428 mmol) was added to a freshly distilled benzene solution (100 ml) of $Os_3(CO)_{10}(MeCN)_2$ (0.200 g, 0.214 mmol) in a 250 ml three-necked round bottom flask. The reaction mixture was heated at 50–60 °C for 5 h. The solvent was removed under reduced pressure and the residue was chromatographed by TLC on silica gel. Elution with hexane/CH_2Cl_2 (10:2, v/v) gave two main bands. The faster moving band gave **4b** (0.037 g, 18%). The slowest moving band yielded **4a** (0.091 g, 45%).

3.12. Reaction of $Ru_3(CO)_{12}$ with 1-vinylimidazole

To a THF solution (25 ml) of $Ru_3(CO)_{12}$ (0.150 g, 0.235 mmol) and 1-vinylimidazole (23 μl, 0.235 mmol) was added three to four drops of a freshly prepared THF solution of sodium benzophenone ketyl. The resulting solution was heated to reflux for 2 h. The progress of the reaction was monitored by spot TLC. The solvent was removed under reduced pressure and the residue was chromatographed by TLC on silica gel. Elution with hexane gave an orange band which yielded (μ-H)$Ru_3(CO)_{10}$(μ-2,3-η^2-$\overline{\text{C=NCH=CHN}}$CH=$CH_2$) (**7**) as orange crystals from pentane at −20 °C (0.035 g, 22%). Anal. Calc. for $C_{15}H_6N_2O_{10}Ru_3$: C, 26.59; H, 0.89; N, 4.14. Found: C, 26.75; H, 0.95; N, 4.20.

3.13. Reaction of $Ru_3(CO)_{12}$ with imidazole

A reaction similar to that above of $Ru_3(CO)_{12}$ (0.150 g, 0.235 mmol) with imidazole (0.016 g, 0.235 mmol) followed by similar chromatographic separation gave (μ-H)$Ru_3(CO)_{10}$(μ-2, 3-η^2-$\overline{\text{C=NCH=CHNH}}$) (**8**) as orange crystals from pentane at −20 °C (0.045 g, 30%). Anal. Calc. for $C_{13}H_4N_2O_{10}Ru_3$: C, 23.97; H, 0.62; N, 4.30. Found: C, 24.35; H, 0.83; N, 4.42.

3.14. X-ray crystallography

Crystals of compounds **2** and **7** for X-ray studies were obtained from saturated solutions of hexane/dichloromethane and pentane respectively at −20 °C. The full details of data collection and structure refinement parameters are listed in Table 2.

3.15. Structure analysis and refinement

Compound **2**: suitable crystals of **2** were mounted on glass fibers, placed in a goniometer head on an Enraf-Nonius CAD4 diffractometer, and centered optically. Unit cell parameters and an orientation matrix for data collection were obtained by using the centering program in the CAD4 system. The intensity data were recorded using an ω-2θ scan method, scan rate 8.23° min^{-1} and scan width (°) = (0.90 + 0.35 tanθ). The actual scan width = scan range + 0.35 tan θ and backgrounds were measured by using the moving crystal-moving counter technique, at the beginning and end of each scan. The structure was solved by the Patterson method using SHELXS-86 [19], which revealed the positions of the osmium atoms. All other non-hydrogen atoms were located in successive difference Fourier synthesis. Hydrogen atoms were positioned using the program HYDRO [20] and included in the structure factor calculations but not refined in the final least-squares cycles. Scattering factors were taken from Cromer and Waber [21]. Anomalous dispersion corrections were those of Cromer [22]. All calculations were carried out on a DEC Micro VAX II computer using the SPD/VAX system of the program. Selected bond length and angles and atom coordinates are given in Tables 3 and 4 respectively.

Compound **7**: the intensity data were collected at 150 K using a Delft Instruments Fast TV area detector diffractometer positioned at the window of rotating anode generator by following previously described procedures [23]. The structure was solved by the routine heavy atom procedures, full matrix least squares refinement on F^2 with all non-hydrogen atoms anisotropic and hydrogen atoms [H(1) free, others in idealized positions] isotropic. All calculations were done on a 486DX2/66 personal computer using the programs SHELXS [19] (solution), SHELXL-93 [24] (refinement) and DIFABS [25] (absorption correction). Sources of scattering factors data were from Ref. [24]. Selected bond lengths and angles, and atom coordinates are given in Tables 5 and 6 respectively.

Acknowledgements

We thank the Royal Society of Chemistry for a research grant (SEK). We also acknowledge the National Science Foundation for research support (E.R. CHE9319062) and for an instrument grant (CHE9302468) for the purchase of a 400-MHz NMR, and the SERC(UK) for support of the crystallographic work at Cardiff.

Supplementary material available

Tables 7 and 8, listing anisotropic displacement parameters, Tables 9 and 10 listing complete bond distances and angles, Tables 11 and 12 listing structure factors for both **2** and **7** and Table 13 listing hydrogen atom parameters for **7**.

References

[1] (a) B.F.G. Johnson, J. Lewis and D.A. Pippard, *J. Chem. Soc., Dalton Trans.,* (1981) 407; (b) B.F.G. Johnson, J. Lewis, T.I. Odiaka and P.R. Raithby, *J. Organomet. Chem., 216* (1981) C56; (c) K. Burgess, B.F.G. Johnson and J. Lewis, *J. Organomet. Chem., 233* (1982) C55.

[2] C.C. Yin and A.J. Deeming, *J. Chem. Soc., Dalton Trans.,* (1975) 2091.

[3] (a) A. Eisenstadt, C.M. Giandomenico, M.F. Frederick and R.M. Laine, *Organometallics, 4* (1985) 2033; (b) R.H. Fish, T. Kim, J.L. Stewart, J.H. Bushweller, R.K. Rosen and J.W. Dupon, *Organometallics, 5* (1986) 2193.

[4] (a) E. Rosenberg, S.E. Kabir, K.I. Hardcastle, M. Day and E. Wolf, *Organometallics, 9* (1990) 2214; (b) M. Day, S. Hajda, S.E. Kabir, M. Irving, T. McPhillips, E. Wolf, K.I. Hardcastle, E. Rosenberg, R. Gobetto, L. Milone and D. Osella, *Organometallics, 10* (1991) 2743; (c) G. Süss-Fink, T. Jenke, H. Heitz, M.A. Pellinghelli and A. Tiripicchio, *J. Organomet. Chem., 379* (1989) 311.

[5] (a) J.R. Shapley, D.E. Samkoff, C. Bueno and M.R. Churchill, *Inorg. Chem., 21* (1982) 634; (b) M.R. Churchill and J.R. Missert, *J. Organomet. Chem., 256* (1983) 349; (c) M. Tachikawa and J.R. Shapley, *J. Organomet. Chem., 124* (1977) C19.

[6] (a) K.A. Azam, A.J. Deeming, I.P. Rothwell, M.B. Hursthouse and J.D.J. Backer-Dirks, *J. Chem. Soc., Dalton Trans.,* (1981) 2039; (b) C.C. Yin, K.A. Azam and A.J. Deeming, *J. Chem. Soc., Dalton Trans.,* (1974) 1013.

[7] A.J. Deeming, R. Peters, M.B. Hursthouse and J.D.J. Backer-Dirks, *J. Chem. Soc., Dalton Trans.,* (1982) 787.

[8] A.J. Deeming, R. Peters, M.B. Hursthouse and J.D.J. Backer-Dirks, *J. Chem. Soc., Dalton Trans.* (1982) 1205.

[9] G.A. Foulds, B.F.G. Johnson and J. Lewis, *J. Organomet. Chem., 296* (1985) 147.

[10] M.I. Bruce, M.G. Humphrey, M.R. Snow, E.R.T. Tiekink and R.C. Wallis, *J. Organomet. Chem., 314* (1986) 311.

[11] F.A. Cotton and D.J. Jamerson, *J. Am. Chem. Soc., 98* (1976) 5396.

[12] J.A. Cabeza, L.A. Oro, A. Tiripicchio and M. Tiripicchio-Camellini, *J. Chem. Soc., Dalton Trans.,* (1988) 1437.

[13] J.A. Cabeza, C. Landazuri, L.A. Oro, A. Tiripicchio and M. Tiripicchio-Camellini, *J. Organomet. Chem., 322* (1987) 111.

[14] G. Süss-Fink, *Z. Naturforsch. Teil B, 35* (1980) 454.

[15] M.R. Churchill and B.G. DeBoer, *Inorg. Chem., 16* (1977) 878.

[16] P.A. Dawson, B.F.G. Johnson, J. Lewis, J. Puga, P.R. Raithby and J. Rosales, *J. Chem. Soc., Dalton Trans.,* (1982) 235.

[17] B.F.G. Johnson, J. Lewis, W.J.H. Nelson, M.A. Pearsall, P.R. Raithby, M.J. Rosales, M. McPartlin and A. Sironi, *J. Chem. Soc., Dalton Trans.,* (1987) 327.

[18] M.I. Bruce, J.G. Matisons and B.K. Nicholson, *J. Organomet. Chem., 247* (1983) 321.

[19] G.M. Sheldrick. *Acta Crystallogr., A46* (1990) 467.

[20] B.A. Frenz, The Enraf-Nonius CAD4SDP - a real-time system for concurrent X-ray data collection and crystal structure Determination, in H. Schenk, R. Ollthof-Hazelkamp, Y. von Konigsveld and G.C. Bassi (eds.), *Computing in Crystallography*, Delft University Press, Delft, 1978.

[21] D.T. Cromer and J.T. Waber, *International Tables for X-ray Crystallography*, Kynoch, Birmingham, Vol. 4, 1974, Table 2.2B.

[22] D.T. Cromer, *International Tables for X-ray Crystallography*, Kynoch, Birmingham, Vol. 4, 1974, Table 2.3.1.

[23] J.A. Darr, S.R. Drake, M.B. Hursthouse and K.M.A. Malik, *Inorg. Chem., 32* (1993) 5704.

[24] G.M. Sheldrick, *J. Applied Crystallog.,* (1994), in preparation.

[25] N.P.C. Walker and D. Stuart, *Acta Crystallogr., A39* (1983) 158; adapted for FAST Geometry by A.K. Karnulov, University of Wales, 1991.